Supporting Information

Optimal Ligand-Receptor Binding for High Efficient Capture of Vesicles in Nanofluidic Transportation

Ziyang Xu, Guolong Zhu, Pengyu Chen, Xiaobin Dai, and Li-Tang Yan*

State Key Laboratory of Chemical Engineering, *Department of Chemical Engineering*,

Tsinghua University, *Beijing 100084*, *P. R. China*

The files include:

Ⅰ. Details of simulation models

As illustrated by the schematic diagram in Fig. S1, the vesicles are formed by self-assembly of amphiphilic molecules, in which the green beads denote hydrophilic head groups and blue beads denote hydrophobic tail groups. Each amphiphilic molecule consists of one hydrophilic bead and three hydrophobic beads.[1,2] The ligand chains are modelled as a series of different beads connected into a chain, which totally include four parts: cholesterol (purple), backbone (cyan), and two types of binding sites (red and yellow), while receptor chains are composed of an anchor bead (purple-blue) at the end and two types of receptor beads (pink and orange) arranged alternately in the head. The hydrophobic cholesterol beads act as anchors and spontaneously insert into the lipid bilayers of the self-assembling vesicles, leaving the other beads pointing outward. A total of thirty ligand chains are grafted and randomly distributed on the surface of the vesicle. Acting as fixed points, the anchor beads enable the receptor chains to be immobilized on the wall of the flow channel.

In order to model the transport process of a vesicle in the channel, we choose a rectangular simulation box with dimensions of $25r_c \times 80r_c \times 25r_c$, for which the periodic boundary condition is set in the direction of the flow (y-axis). The diameter of the cylindrical channel is $24r_c$, with the length being the same with that of the y-axis. The cylinder channel is made of a single layer of frozen DPD beads, which can interact with other beads but are not allowed to move. We keep the wall density the same with the fluid density, as the significantly enlarged wall density will cause distinct density fluctuations across the channel. Due to the soft interaction between DPD beads, the bounce-back boundary condition is necessary to be imposed on the surface of the wall with half inter-beads distance ($0.5\rho^{-\frac{1}{3}}$) to

prevent beads from penetrating it.[3] When a DPD beads approach the surface of the wall, its tangential and normal velocity component are both reversed. This imposed bounce-back reflection is effective to reflect the beads back into the fluid, which is confirmed by Pivkin et.al.[3] A bead density of $\rho = 3r_c^{-3}$ is set, so that the total number of beads in the system is 150000. By adding the body force F_b to all solvent beads outside the vesicles along the long axis of the channel, we can simulate the Poiseuille flow through the channel.[4] In the beginning of the simulations, we place the ligand-functionalized vesicle on one side of the cylindrical channel, which is surrounded by solvent beads. During the first 100τ (t_0) of the simulation, the body force is fixed at 0. Then, the force F_b gradually increases with time, satisfying the formula $F_b = F_0\left(t/t_0 - 1\right)$. The purpose is to prevent the vesicle from rupturing due to the sudden application of the flow field. When simulation time t=200τ, the body force F_b reaches the maximum value F_0, and it remains constant until the end of the simulation.

Ⅱ. Details of DPD simulations

In this study, our coarse-grained simulations are on the basis of the dissipative particle dynamics (DPD), a method that samples the NVT ensemble. Taking into account the limitation in the time and length scales in simulation, the DPD simulation method bridges the gap between atomistic and mesoscopic simulation, and thereby it has been broadly used in many areas.[5-7] In DPD simulations, each bead represents clusters of molecules, where the position of the bead represents the mass center of the clusters. The time evolution of positions and velocities is governed by Newton's motion equations as follow

$$\frac{d\mathbf{r}_i}{dt} = \mathbf{v}_i, \quad \frac{d\mathbf{v}_i}{dt} = \mathbf{f}_i + \mathbf{F}_e \tag{1}$$

where the $\mathbf{r}_i$ and $\mathbf{v}_i$ represent the position and the velocity vectors of beads i, and $\mathbf{F}_e$ is the external force. For simplicity, the masses of the particles are set as 1. The beads i and j experience a force with the component of conservative force $\mathbf{F}^{\mathrm{C}}$, dissipative force $\mathbf{F}^{\mathrm{D}}$, and random force $\mathbf{F}^{\mathrm{R}}$, i.e., $\mathbf{f}_i = \sum_{j \neq i} \left(\mathbf{F}_{ij}^C + \mathbf{F}_{ij}^D + \mathbf{F}_{ij}^R \right)$, where the pairwise interaction forces are truncated within a certain cutoff radius r_{c}. We take r_{c} as our characteristic length scale and set the dimensionless value as r_{c}=1. The conservative force is a soft repulsion and is given by

$$\mathbf{F}_{ij}^C = \begin{cases} a_{ij}(1 - r_{ij})\hat{\mathbf{r}}_{ij} & (r_{ij} > 1) \\ 0 & (r_{ij} \geq 1) \end{cases} \tag{2}$$

where $\mathbf{r}_{ij} = \mathbf{r}_i - \mathbf{r}_j$, $r_{ij} = \left| \mathbf{r}_{ij} \right|$, and $\hat{\mathbf{r}}_{ij} = \mathbf{r}_{ij} / |\mathbf{r}_{ij}|$. a_{ij} is the maximum repulsion between beads i and j, which has a linear relationship with Flory-Huggins χ parameter as

$$\chi_{ij} \approx \frac{\left(a_{ij} - a_{ii} \right)}{3.27} \tag{3}$$

where a_{ii}=25 is the repulsion parameter between the same beads in our simulation system (*i.e.*, $\chi_{ii} = 0$). a_{ij} will be smaller than 25 for a strong attraction between two beads while it will be larger than 25 for a strong bead-bead repulsion interaction. The larger the value of a_{ij}, the greater the repulsive force between beads i and j and vice versus. Here, each parameter is selected carefully based on the properties and interactions of different beads. We set a_{HT}= a_{TW} =100, a_{HW} =20, a_{LR}=15, where the subscript H and T respectively represent the head and tail part of the amphiphilic molecules, L and R are the binding sites of the ligand and receptor chains, and W represents solvent.

The dissipative force and the random force act together as a thermostat and are given by

$$\mathbf{F}_{ij}^D = -\gamma \omega^D(r_{ij})(\hat{\mathbf{r}}_{ij} \cdot \mathbf{v}_{ij})\hat{\mathbf{r}}_{ij} \tag{4}$$

$$\mathbf{F}_{ij}^R = \sigma \omega^R(r_{ij}) \zeta_{ij} \Delta t^{-1/2} \hat{\mathbf{r}}_{ij} \tag{5}$$

where $\mathbf{v}_{ij} = \mathbf{v}_i - \mathbf{v}_j$; ω^D and ω^R are weight functions and conform to the formula $\omega^D(r_{ij}) = [\omega^R(r_{ij})]^2 = (1-r_{ij})^2$ for r_{ij}<1; ζ_{ij} is a random number with zero mean and unit variance; Δt is the time step in simulation; γ is a simulation parameter related to viscosity and the noise amplitude satisfies $\sigma^2 = 2\gamma k_B T$. k_B and T respectively represent Boltzmann constant and the temperature. $k_B T = 1$ is set in the study. The characteristic time scale is defined as $\tau = \sqrt{m r_c^2 / k_B T}$. The remaining simulation parameters are $\gamma = 4.5$ and $\sigma = 3$. All simulations are based on a modified version of the velocity-Verlet algorithm as follows

$$\begin{aligned} \mathbf{r}_i(t+\Delta t) &= \mathbf{r}_i(t) + \Delta t \mathbf{v}_i(t) + \frac{1}{2}(\Delta t)^2 \mathbf{f}_i(t) \\ \tilde{\mathbf{v}}_i(t+\Delta t) &= \mathbf{v}_i(t) + \lambda \Delta t \mathbf{f}_i(t) \\ \mathbf{f}_i(t+\Delta t) &= \mathbf{f}_i(\mathbf{r}(t+\Delta t), \tilde{\mathbf{v}}(t+\Delta t)) \\ \mathbf{v}_i(t+\Delta t) &= \mathbf{v}_i(t) + \frac{1}{2}\Delta t(\mathbf{f}_i(t) + \mathbf{f}_i(t+\Delta t)) \end{aligned} \tag{6}$$

To assure the accurate temperature control of the simulation system, we set $\Delta t = 0.01\tau$ as the time step and select the bead number density of $3r_c^{-3}$.

Ⅲ. Details of the analytical model of Blob theory

We develop the blob theory[8,9] for the dependence of the binding stability on the chain stiffness.

For wormlike chain model, the tangent vector correlation function can be expressed as

$$< \vec{t}(s) \cdot \vec{t}(s) >= e^{-|s-s'|/l_p} \tag{1}$$

which leads to the mean-squared end to end distance

$$< R^2 >= \int_0^L ds \int_0^L ds' < \vec{t}(s) \cdot \vec{t}(s') >= \int_0^L ds \int_0^L ds' e^{-|s-s'|/l_p} \tag{2}$$

This is the famous Debye integral. Through integrating, we can get

$$< R^2 >= 2l_pL\left[1-\frac{l_p}{L}\left(1-e^{-L/l_p}\right)\right] \tag{3}$$

where L represents the chain contour length. In our system, the contour length of the ligand and receptor chains are set as $L_1 = 4.7r_c$ and $L_2 = 4.1r_c$ respectively. In the flexible chain limit of $l_p \to 0$, it has $< R^2 >\approx 2l_pL$, which gives the Gaussian chain limit. In the rigid chain limit of $l_p \to \infty$, it has $< R^2 >\approx L^2$, which is the rod-like limit. It is consistent with the actual situation, which proves the correctness of the equation. Following the Ornstein-Zernike approximation, we approximate Equation (3) as

$$< R^2 >\approx \frac{L^2}{1+\left(L/l_p\right)/2} \tag{4}$$

In our study, we define the average chain length of the ligand and receptor chains as H. It is clearly that H is a function of the chain stiffness characterized by the persistence length l_p, while H monotonically increases as the persistence length l_p increases.

We define the area density of grafted chains as σ, satisfying $\sigma \approx d^{-2}$, where d is the average distance among grafted chains. In blob theory, we hypothesis a grafted chain consist of N/g blobs of size d, where N represents the number of statistical segment of a single chain and g is the number of segment contained in a blob. So the average length of the ligand or receptor chains can be expressed as $H = \frac{N}{g}d$. In order to explain the effects of the chain stiffness, we need to further analyze this expression.

According to the above analysis of the wormlike chain model, combined with Equation (4), we have

$$d^2 = \frac{(ga)^2}{1+\left(ga/l_p\right)/2} \tag{5}$$

where a is the statistical segment length. Solving the above equation, we get the relation between g and d

$$g = \frac{d^2}{4l_p a}\left[1+\sqrt{1+\frac{16l_p^2}{d^2}}\right] \tag{6}$$

Let's check the limit. For the flexible chain limit of $l_p \to 0$, we have

$$g \approx \frac{d^2}{4l_p a}\left[1+\sqrt{1}\right] = \frac{d^2}{2l_p a} \tag{7}$$

While, for the rigid chain limit of $l_p \to \infty$, we have

$$g \approx \frac{d^2}{4l_p a}\left[1+\frac{4l_p}{d}\right] \approx \frac{d}{a} \tag{8}$$

The expression $d = ga$ is exactly the rod statistics. With the Equation (6), we can derive the average length of the ligand or receptor chains as

$$H = \frac{N}{g}d = \frac{4Ll_p\sigma^{1/2}}{1+\sqrt{1+16\sigma l_p^2}} \tag{9}$$

The two limits are easy to be checked. For the flexible chain limit of $l_p \to 0$, it has $H = 2Ll_p\sigma^{1/2}$. For the rigid chain limit of $l_p \to \infty$, it has $H = L$,which is independent of the area density of grafted chains. In our system, we set $\sigma \approx 0.318 r_c^{-2}$, and the dependence of average chain length on chain stiffness is shown in Fig. 6a in the main paper.

The average length of the ligand and the receptor chains can be expressed as H_1 and H_2, respectively. As shown in Fig. S5, H is a function of the chain stiffness characterized by the persistence length l_p, which monotonically increases with the increase of l_p. Throughout the transport process, as the ligand-functionalized vesicle approaches the receptor area in the channel, the ligand and the receptor chains have a certain probability of recognition and binding, depending on the relative positions of the end groups (binding sites) of ligands and

receptors. We define the sum of the average length of the ligand (H_1) and receptor (H_2) chains as L_t, i.e., $L_t = H_1 + H_2$, which can be expressed as an equation related to the persistence length of ligand (l_{p1}) and receptor (l_{p2}) chains as follows

$$L_t = \frac{4L_1 l_{p_1} \sigma^{1/2}}{1+\sqrt{1+16\sigma l_{p_1}^2}} + \frac{4L_2 l_{p_2} \sigma^{1/2}}{1+\sqrt{1+16\sigma l_{p_2}^2}} \tag{10}$$

Therefore, we can obtain the relation between l_{p1} and l_{p2} with different values of L_t based on Equation (10). As shown in the inset of Fig. 1c, the maximum binding probability can be realized when the three binding site beads of a ligand totally bind with those of a receptor.

Ⅳ. Supplementary figures

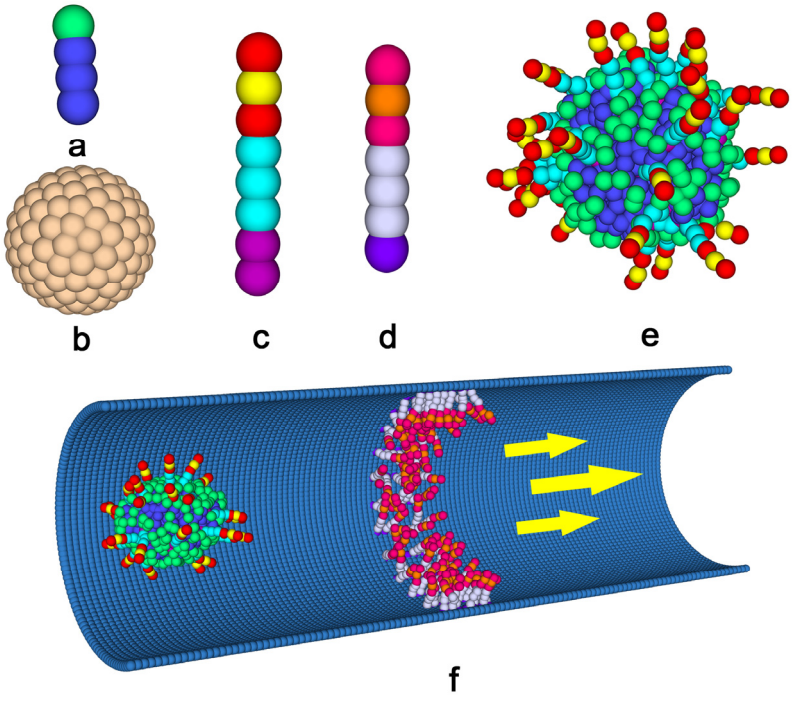

Figure S1. Schematic illustration of the coarse-grained models for (a) amphiphilic molecules, (b) rigid sphere, (c) ligand chain, (d) receptor chain, and (e) ligand-modified vesicle. (f) Schematic representation of a ligand-functionalized vesicle transporting through a cylindrical channel, where the yellow arrows indicate the direction of the flow in the channel. Solvent beads are not shown for clarity.

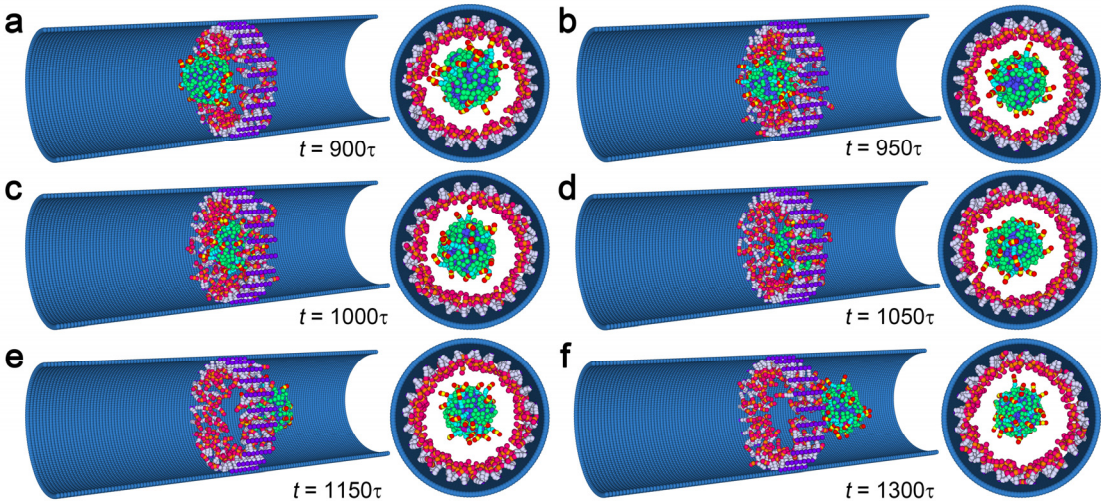

Figure S2. Representative snapshots demonstrate the detailed dynamic process of flow-induced transport of ligand-functionalized vesicle at K1=K2=10kBT. The snapshots are taken for times (a) 900τ, (b) 950τ, (c) 1000τ; (d) 1050τ, (e) 1150τ, and (f) 1300τ, and the Re is fixed at 1.8 for this system.

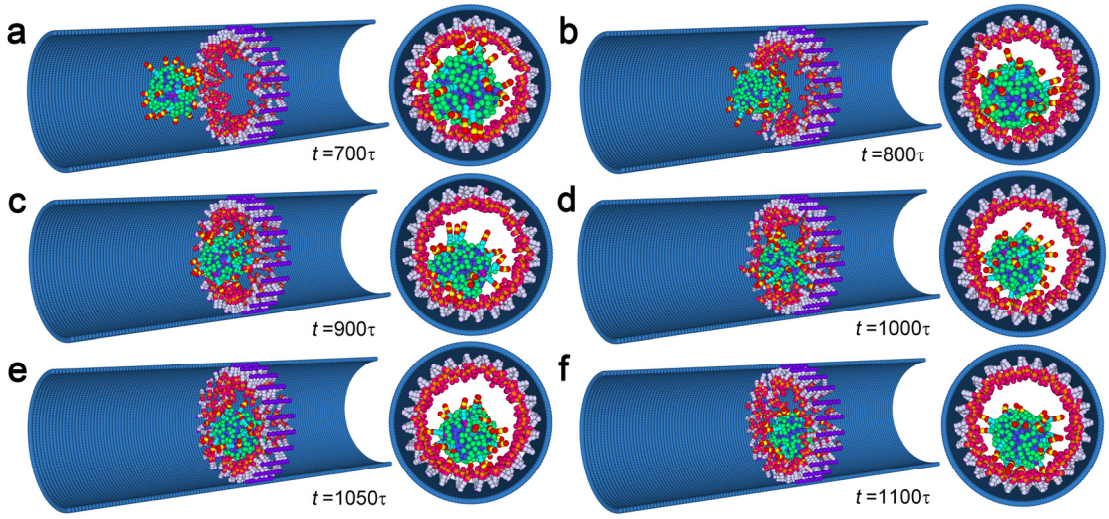

Figure S3. Representative snapshots demonstrate the detailed dynamic process of flow-induced transport of ligand-functionalized vesicle at K1=K2=70kBT. The snapshots are taken for times (a) 700τ, (b) 800τ, (c) 900τ; (d) 1000τ, (e) 1050τ, and (f) 1100τ, and the Re is fixed at 1.8 for this system.

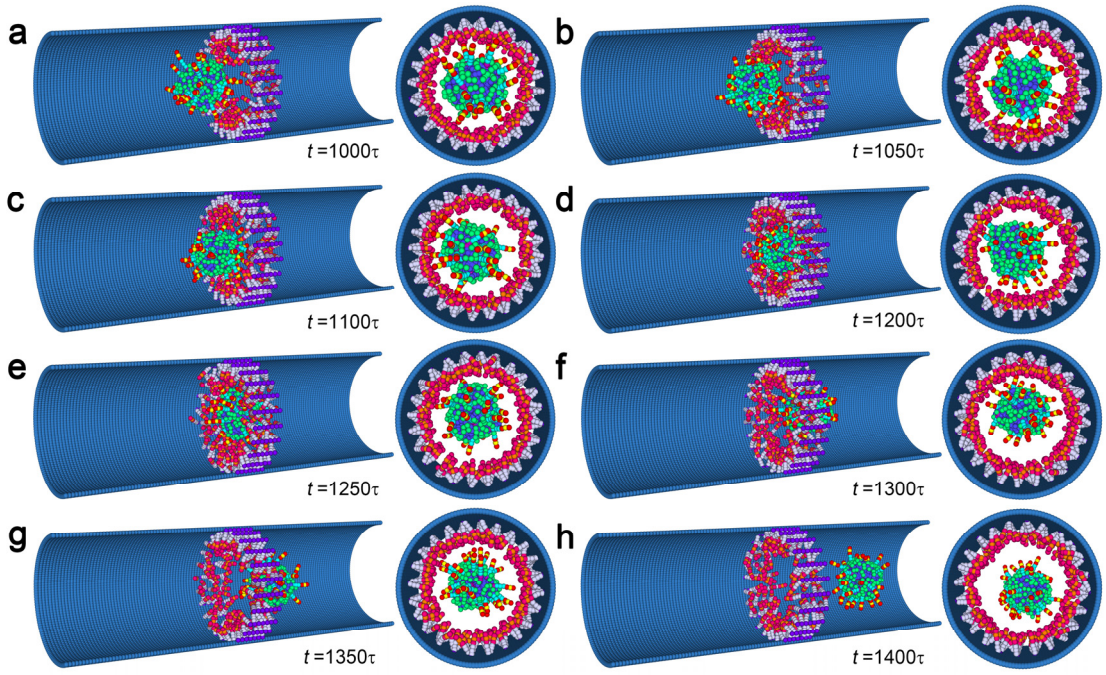

Figure S4. Representative snapshots demonstrate the detailed dynamic process of flow-induced transport of ligand-functionalized vesicle at K1=K2=120kBT. The snapshots are taken for times (a) 900τ, (b) 950τ, (c) 1000τ; (d) 1050τ, (e) 1150τ, and (f) 1300τ, and the Re is fixed at 1.8 for this system.

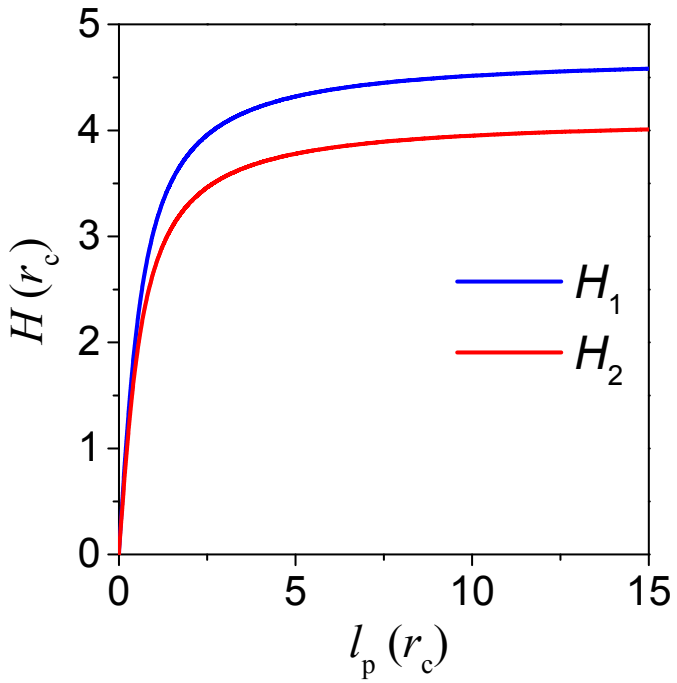

Figure S5. Dependence of average chain length on chain stiffness. With increasing the persistence length, the average chain length increases monotonically and finally approaches the contour length of the chain. The area density of grafted chains is set to be σ=0.318 chains/r_c^2 and the contour length of the ligand and receptor chains are 4.7r_c and 4.1r_c, respectively.

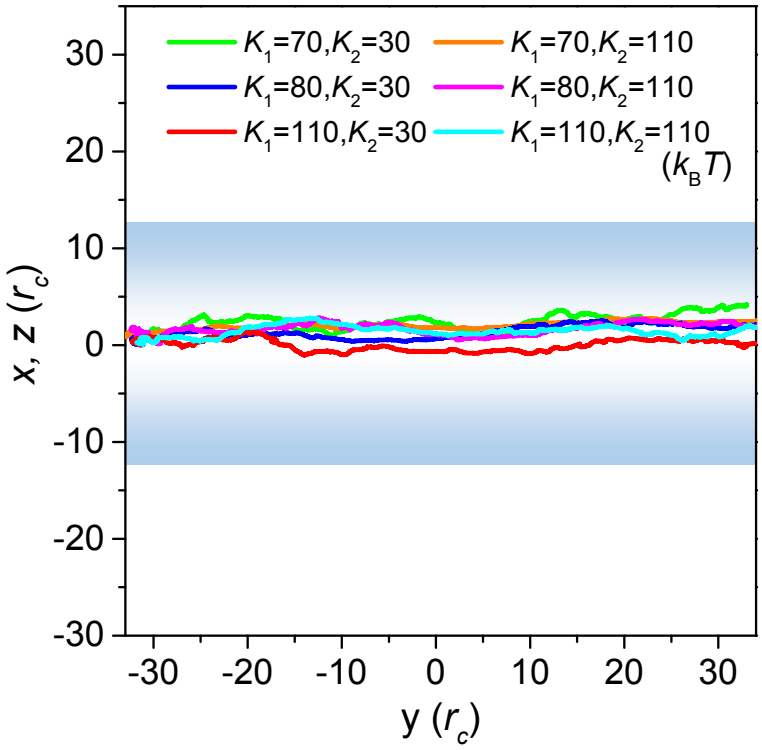

Figure S6. Representative motion trajectories of flow-induced transport of the ligand-functionalized hard vesicles for 6 groups of ligand and receptor stiffness: K_1=70 k_BT at K_2=30 k_BT and K_2=110 k_BT; K_1=80 k_BT at K_2=30 k_BT and K_2=110 k_BT; K_1=110 k_BT at K_2=30 k_BT and K_2=110 k_BT. The Re is set as 1.8.

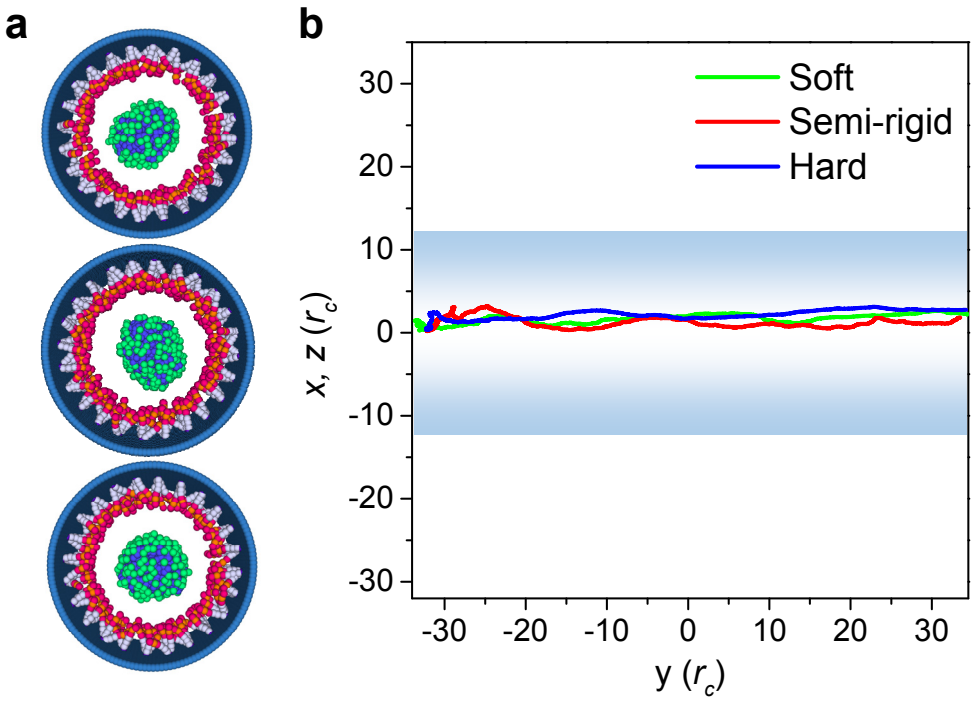

Figure S7. Transport behavior of pure vesicles with different rigidities in the flow channel. (a) Snapshots showing the transport process of soft (top), semi-rigid (middle), and hard (bottom) pure vesicles. (b) Representative motion trajectories of pure vesicles with different rigidities in the flow channel, where Re=1.8.

Ⅴ. Supplementary Videos

Supplementary Video S1. The detailed dynamic process of the direct pass regime under the condition of flexible ligand and receptor chains (K_1=10k_BT and K_2=10k_BT).

Supplementary Video S2. The detailed dynamic process of the capture regime under the condition of semiflexible ligand and receptor chains (K_1=70k_BT and K_2=70k_BT).

Supplementary Video S3. The detailed dynamic process of the direct pass regime under the condition of stiff ligand and receptor chains (K_1=120k_BT and K_2=120k_BT).

Supplementary Video S4. The detailed dynamic process of the rearrangement of ligand-receptor binding (K_1=100k_BT and K_2=100k_BT).

Ⅵ. References

1. S. Yamamoto, Y. Maruyama and S. A. Hyodo, *J. Chem. Phys*., 2002, **116**, 5842-5849.

2. M. Dutt, O. Kuksenok, M. J. Nayhouse, S. R. Little and A. C. Balazs, *ACS Nano*, 2011, **5**, 4769-4782.

3. I. V. Pivkin, G. E. Karniadakis, *J. Comput. Phys.*, 2005, **207**, 114-128.

4. X. Chu, X. Yu, J. Greenstein, F. Aydin, G. Uppaladadium and M. Dutt, *ACS Nano*, 2017, **11**, 6661-6671.

5. R. D. Groot and P. B. Warren, *J. Chem. Phys.,* 1997, **107**, 4423-4435.

6. P. B. Warren, *Phys. Rev. E*, 2003, **68**, 066702.

7. R. D. Groot and T. J. Madden, *J. Chem. Phys.*, 1998, **108**, 8713-8724.

8. G. Xu, Z. Huang, P. Chen, T. Cui, X. Zhang, B. Miao and L. T. Yan, *Small*, 2018, **13**, 1603155.

9. P. G. de Gennes and *Macromolecules,* 1980, **13**, 1069-1075.